Development 138, 5067-5078 (2011) doi:10.1242/dev.074591


# The role of Pax6 in regulating the orientation and mode of cell division of progenitors in the mouse cerebral cortex

**Maki Asami[1], Gregor A. Pilz[1], Jovica Ninkovic[1,4], Leanne Godinho[2], Timm Schroeder[1], Wieland B. Huttner[3] and Magdalena Götz[1,4,*]**

## SUMMARY

Successful brain development requires tight regulation of sequential symmetric and asymmetric cell division. Although Pax6 is known to exert multiple roles in the developing nervous system, its role in the regulation of cell division is unknown. Here, we demonstrate profound alterations in the orientation and mode of cell division in the cerebral cortex of mice deficient in Pax6 function ($Pax6^{Sey/Sey}$) or after acute induced deletion of Pax6. Live imaging revealed an increase in non-vertical cellular cleavage planes, resulting in an increased number of progenitors with unequal inheritance of the apical membrane domain and adherens junctions in the absence of Pax6 function. This phenotype appears to be mediated by the direct Pax6 target Spag5, a microtubule-associated protein, reduced levels of which result in the replication of the Pax6 phenotype of altered cell division orientation. In addition, lack of Pax6 also results in premature delamination of progenitor cells from the apical surface due to an overall decrease in proteins mediating anchoring at the ventricular surface. Moreover, continuous long-term imaging in vitro revealed that Pax6-deficient progenitors generate daughter cells with asymmetric fates at higher frequencies. These data demonstrate a cell-autonomous role for Pax6 in regulating the mode of cell division independently of apicobasal polarity and cell-cell interactions. Taken together, our work reveals several direct effects that the transcription factor Pax6 has on the machinery that mediates the orientation and mode of cell division.

**KEY WORDS: Radial glia, Asymmetric cell division, Neurogenesis, Spag5**

## INTRODUCTION

The mammalian neocortex develops from a pseudostratified neuroepithelium by progressive cell divisions of neuroepithelial cells and radial glia (Götz and Huttner, 2005). Before the onset of neurogenesis, neuroepithelial cells divide mostly in a symmetric manner to yield exponential progenitor production and tangential growth of the cortex. During neurogenesis, asymmetric cell divisions take over, producing either one neuron or a neurogenic basal progenitor in addition to self-renewal (for a review, see Götz and Huttner, 2005; Kriegstein et al., 2006; Miyata, 2007). Thus, asymmetric cell divisions lead to radial growth of the cerebral cortex, whereas symmetric cell divisions regulate the tangential size of the cerebral cortex (Rakic, 2009; Farkas and Huttner, 2008). Despite the importance of these parameters in mammalian evolution (Molnar et al., 2006; Fish et al., 2008), little is known about the molecular machinery regulating the mode of cell division in the developing cerebral cortex in mammals.

By contrast, in *Drosophila*, the mechanisms of asymmetric cell division are known at high resolution, with a clear link between cleavage plane orientation and asymmetric inheritance of proteins (for reviews, see Matsuzaki, 2000; Doe, 2008; Knoblich, 2008). However, in vertebrate neurogenesis, the link between orientation of cell division and fate of the daughter cells is not as close. For example, in chick and mice, mis-orientation of spindles does not automatically influence cell fate as demonstrated by experimental manipulation of Leu-Gly-Asn repeat-enriched protein (LGN) (Morin et al., 2007; Konno et al., 2008). Moreover, basal localization of the fate determinant Trim32 is independent of spindle orientation (Schwamborn et al., 2009; Godin et al., 2010) and the inheritance of adherens junction or apical membrane components depends on the cleavage furrow (Huttner and Kosodo, 2005; Marthiens and ffrench-Constant, 2009). Finally, daughter cells with asymmetric fates can arise from vertical cell divisions and daughters inheriting the apical domain can become either progenitors or neurons (Wilcock et al., 2007; Alexandre et al., 2010).

To gain new insights into the regulation of the mode of cell division in vertebrate neural development, we took a different approach by examining the role of the transcription factor Pax6, a known regulator of neurogenesis and proliferation (Götz et al., 1998; Warren et al., 1999; Osumi, 2001; Heins et al., 2002; Stoykova et al., 2003; Haubst et al., 2004; Berger et al., 2007; Quinn et al., 2007; Osumi et al., 2008; Sansom et al., 2009). Intriguingly, previous analysis of the cerebral cortex of mice lacking functional Pax6, such as *small eye* (*Sey*) homozygous mutants ($Pax6^{Sey/Sey}$) (Hill et al., 1991) reported a decreased tangential expansion of the $Pax6^{Sey/Sey}$ cerebral cortex (Schmahl et al., 1993), which might be linked to the alterations in the orientation of cell divisions reported previously (Estivill-Torrus et al., 2002). We therefore set out to determine this as yet relatively unexplored role of Pax6.

## MATERIALS AND METHODS

### Animals

*Small eye* (*Sey*, designated $Pax6^{Sey}$) mutant mice (Hill et al., 1991) were maintained on a C57BL/6J × DBA/2J (B6D2F1) background, with a 12 hour light-dark cycle and were also crossed with Tis21::GFP (Haubensak

[1]Institute for Stem Cell Research, Helmholtz Zentrum München German Research Center for Environmental Health, Ingolstädter Landstr. 1, 85764 Neuherberg/Munich, Germany. [2]Biomolecular Sensors, Institute of Neuroscience, Technical University Munich, Biedersteinerstr. 29, 80802 Munich, Germany. [3]Max-Planck Institute of Molecular Cell Biology and Genetics, Pfotenhauerstr. 108, 01307 Dresden, Germany. [4]Physiological Genomics, Ludwig-Maximilians University of Munich, Schillerstr. 46, 80639 Munich, Germany.

*Author for correspondence (magdalena.goetz@helmholtz-muenchen.de)

**Accepted 21 September 2011**

et al., 2004) or YVI mice (George et al., 2007). The day of the vaginal plug was considered as embryonic day (E) 0. For conditional deletion of *Pax6* we used $Pax6^{flox/flox}$ mice (Ashery-Padan et al., 2000).

### Immunocytochemistry and immunohistochemistry

Brains isolated from E12-16 embryos were fixed in 4% (w/v) paraformaldehyde (PFA) in phosphate buffered saline (PBS), cryoprotected in 30% (w/v) sucrose in PBS, embedded in Tissue-Tek and cryosectioned (20-40 μm). Cultured cells were fixed and stained as described previously (Haubst et al., 2004) with the following primary antibodies: anti-ASPM (rabbit, 1:1000) (Fish et al., 2006); anti-βIII-tubulin (mouse IgG2b, Sigma, 1:200); anti-MAP2 (mouse IgG1, Sigma, 1:200); anti-GFP (chicken, Sigma, 1:1000); anti-Pax6 [rabbit, Chemicon, 1:400; mouse, Developmental Studies Hybridoma Bank (DSHB), 1:70]; anti-Pard3 (rabbit, Upstate, 1:500); anti-aPKC (mouse, BD Transduction, 1:200); anti-N cadherin (mouse, BD Transduction, 1:1000); anti-β catenin (mouse, BD Transduction, 1:1000; rabbit, Sigma, 1:2000); anti-phosphohistone H3 (PH3, rabbit, Biomol, 1:400); anti-Ngn2 (mouse, provided by D. Anderson, California Institute of Technology, Pasadena, CA, USA, 1:10); anti-Mash1 (mouse, DSHB, 1:150) and anti-Spag5 (rabbit, AB BioTech, 1:200). After staining with fluorescently labelled secondary antibodies, nuclei were labelled by incubation in PBS containing 0.1 μg/ml DAPI (4′,6-diamidino-2-phenylindole, Sigma), and samples were mounted in Aqua Polymount (Polyscience) and analyzed using Olympus FV1000 confocal laser scanning microscopes. Fluorescence-activated-cell-sorting (FACS) based on anti-prominin 1 staining (PE-conjugated, e-Bioscience, 1:400; supplementary material Fig. S4) was performed as previously described (Pinto et al., 2008).

### In utero electroporation and en face and sliced cortices live imaging

Pregnant mice were operated as approved by the Government of Upper Bavaria under licence number 55.2-1-54-2531-144/07 and were anaesthetized by intraperitoneal (i.p.) injection of saline solution containing fentanyl (0.05 mg/kg), midazolam (5 mg/kg) and medetomidine (0.5 mg/kg) and E12-13 embryos were electroporated as described by Saito (Saito, 2006). Plasmids pCAG-ZO1-EGFP, pCAG-PACT-mKO1 [gifts from Dr F. Matsuzaki; mKO1 (Medical and Biological Laboratories)] (Konno et al., 2008), pCIG2-CAG (cytoplasmic GFP; gift from Dr C. Schuurmans) (Hand et al., 2005) and pCAGGs-GAP43-GFP (Attardo et al., 2008) were dissolved in saline to give a final concentration of 1 μg/μl and co-introduced with Fast Green (2.5 μg/μl, Sigma). Electric pulses were generated by ElectroSquireportator T830 (Harvard Apparatus) and applied five times at ~40 mV for 50 msec each at intervals of 100 msec. Anaesthesia was terminated by i.p. injection of saline solution containing buprenorphine (0.1 mg/kg), atipamezol (2.5 mg/kg) and flumazenil (0.5 mg/kg). Animals recovered well after the operation and no signs of distress could be observed one day later. The tissues for en face imaging were prepared as described previously (Konno et al., 2008). Slices of the embryonic brains were cut 1 day later at a thickness of 300 μm using a vibratome (Leica VT1200S), embedded into collagen matrix (Nitta Gelatin, Cell Matrix type A) and subsequently covered with neurobasal medium (Gibco) with supplements (Polleux and Ghosh, 2002). Images were captured every 8 minutes for en face imaging using a confocal microscope (Olympus Fluoview 1000) or every 20 minutes for slice imaging using an Olympus microscope Fluoview 1000 equipped with a Ti:sapphire Laser tuned to 880 nm to excite GFP fluorescent protein and analyzed using Olympus FV10-ASW1.7 Viewer software and ImageJ (http://rsbweb.nih.gov/ij).

### Continuous live imaging of cortical progenitors in vitro

The cerebral cortex was dissected from E13 or E14 embryos, dissociated and cultured as described previously (Costa et al., 2008). Using cell observer (Zeiss), images were acquired every 4 minutes for phase contrast and every 3 hours for fluorescence for 4-7 days using Axiovision Rel. 4.5 software. Data was analyzed using TTT tracking software as previously described (Costa et al., 2008; Rieger et al., 2009).

### Ratiometric semi-quantitative PCR (qPCR)

Total RNA was extracted from E12 or E15 cerebral cortices using RNAeasy mini kit (QIAGEN) followed by reverse transcription to cDNA using SuperScript II Kit (Invitrogen). Real-time PCR was performed by using the DNA Engine Opticon (Bio-Rad Laboratories) and SYBR Green qPCR kit (Bio-Rad) in triplicate at 95°C for 15 minutes, followed by 40 cycles consisting of 94°C for 15 seconds, primer annealing at the optimal temperature for 30 seconds and primer extension at 72°C for 30 seconds. A melting curve analysis was performed from 70°C to 95°C in 0.3°C intervals to demonstrate the specificity of each amplicon and to identify the formation of primer dimers. Gapdh was used to normalize for differences in RNA input. Relative expression of each mRNA was calculated using the ΔCt between the gene of interest and Gapdh ($E=2^{-\Delta\Delta Ct}$). Primers are shown in supplementary material Table S1.

### Luciferase assay

Expression plasmids for luciferase reporter assays were constructed using full-length cDNA of mouse *Pax6* (Ninkovic et al., 2010) sub-cloned into the pCAG vector. The empty vector was used as control. The *Spag5* promoter (601 bases) was cloned into the pGL3 vector (Promega). The *Spag5* promoter was PCR amplified from genomic DNA using the following primers: 5′-GCGAAGGCGACAAACCGAGA-3′ and 5′-AGTGGTGGTGTGGGACACGCTGTT-3′. HEK293 cells were transfected with 1 μg expression plasmid, 1.5 μg of the construct containing the *Spag5* promoter driving firefly (*Photinus pyralis*) luciferase and 0.1 μg of the pRL-TK plasmid encoding *Renilla* (sea pansy, *Renilla reniformis*) luciferase (Promega). After 24 hours, medium was changed and cell extracts were prepared the following day for luciferase activity measured with a luminometer (Berthold Centro LB 960) and relative light units were normalized to *Renilla* luciferase activity and then to the control transduced cells.

### Chromatin immunoprecipitation (ChIP)-qPCR assay

The qChIP experiments were performed as described elsewhere (Lee et al., 2006) with minor modifications. Chromatin was extracted from E14 mouse cortices and crosslinked, then the Pax6-binding chromatin fragments were immunoprecipitated using polyclonal Pax6 antibodies (rabbit, Chemicon), with pre-immune serum as control (each 5 μg antibody per immunoprecipitation). The immunoprecipitated fragments were purified and amplified for promoter-specific analysis of Spag5 using real-time PCR. Data were normalized using the percent input method (Carey et al., 2009).

### shRNA-mediated Spag5 knockdown

The pSuper.gfp/neo-Spag5 construct was generated by digesting the pSuper.gfp/neo vector (Oligoengine) with *Bgl*II and *Hin*dIII and ligating the annealed oligonucleotides (modified from TRCN0000120646:Sigma; top strand, 5′-GATCCCCCCTAACAGAAATTGTTGCTATTCAAGAGA-TAGCAACAATTTCTGTTAGGTTTTTA-3′; bottom strand, 5′-AGCT-TAAAAACCTAACAGAAATTGTTGCTATCTCTTGAATAGCAACA-ATTTCTGTTAGGGGG-3′) that contain a 20-nucleotide *Spag5* target sequence (in cap) using the strategy according to the manufacturer's instructions. The pSuper.gfp/neo-Spag5 (Spag5-shRNA) and blank vector pSuper.gfp/neo as a control were in utero electroporated into E12 wild-type (WT) cerebral cortices and the effect on the cleavage angles of progenitors was analyzed at E14.

### Data analysis

Quantitative data are depicted as mean with standard error of the mean (s.e.m.) obtained from least three culture batches or embryos tested for significance by the unpaired Student's *t*-test or one-way ANOVA.

## RESULTS

### Alterations in the orientation of apical progenitor cell division in the $Pax6^{Sey/Sey}$ cerebral cortex

To gain a better understanding of the characteristics of cell division in $Pax6^{Sey/Sey}$ mutants, we first examined the cleavage angles of progenitor cells dividing at the apical surface in wild-type (WT) and $Pax6^{Sey/Sey}$ cerebral cortices at an embryonic stage

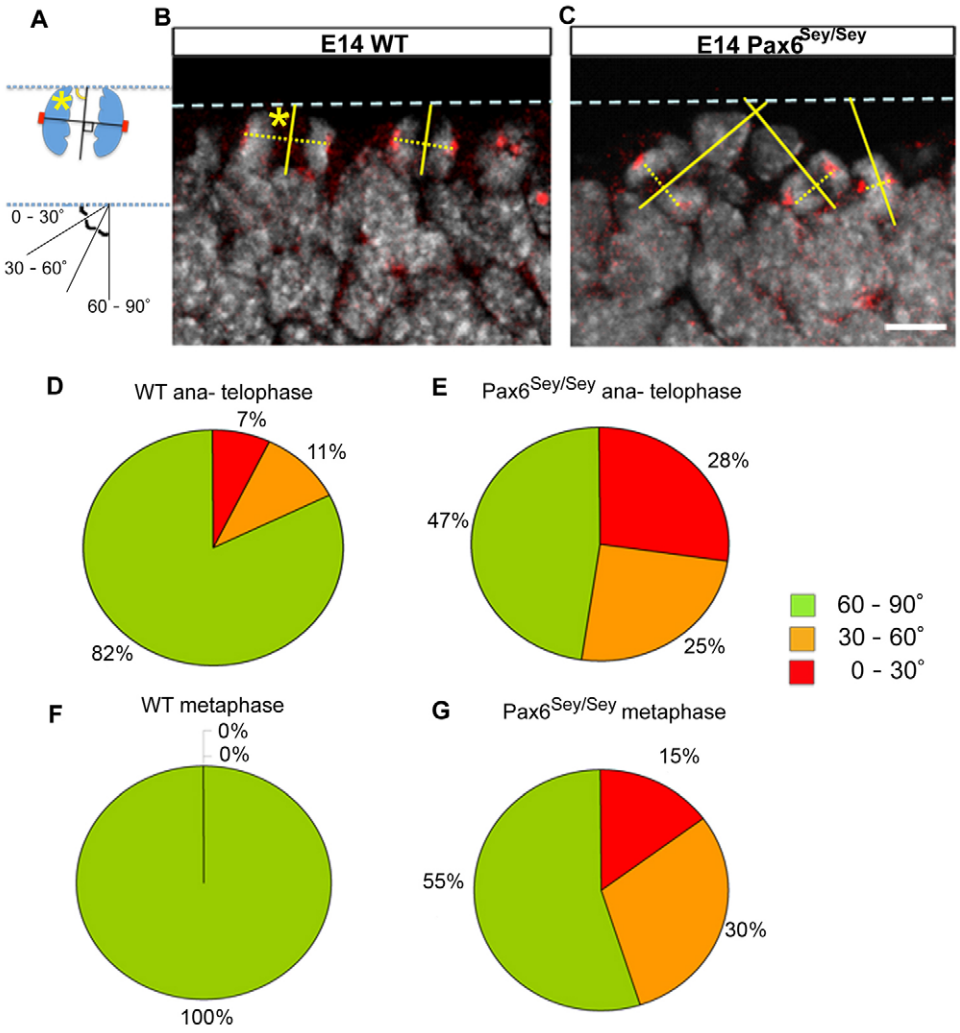


**Fig. 1. Apical progenitors often divide non-vertically in mouse Pax6$^{Sey/Sey}$ cerebral cortex at mid-neurogenesis.** (**A**) The cleavage angles (yellow asterisk) were measured as shown schematically and grouped into vertical (60-90°), oblique (30-60°) and horizontal (0-30°). (**B**,**C**) Cells labelled for ASPM (red) and DAPI+ nuclei (grey) at the apical surface (dashed line) of coronal sections of E14 WT (B) or Pax6$^{Sey/Sey}$ (C) cerebral cortices. (**D-G**) Pie charts showing the percentage of cells with the colour coded cleavage angle for ana- and telophase (D,E) and for metaphase (F,G) of WT (D,F; 81 cells from three animals) or Pax6$^{Sey/Sey}$ (E,G; 129 cells from three animals). Scale bar: 10 μm.

corresponding to mid-neurogenesis in the mouse (E14). In WT cortices immunostained for the mitotic spindle pole protein Aspm (abnormal spindle-like microcephaly associated), we noted that the spindles of most apically dividing cells (neuroepithelial or radial glia cells) at anaphase were oriented along a horizontal plane (Fig. 1A,B, dashed yellow line) in accordance with previous observations (Chenn and McConnell, 1995; Estivill-Torrus et al., 2002; Kosodo et al., 2004; Stricker et al., 2006; Fish et al., 2006; Konno et al., 2008). In these divisions, the spindle axis is almost parallel to the ventricular, apical surface and the cleavage plane is, accordingly, vertical to the ventricular lining (Fig. 1A). The observed angles of cell divisions were grouped into three classes, with a cleavage plane angle of 60-90° (relative to the apical surface of the cortex) scored as vertical, 30-60° as oblique and 0-30° as horizontal (Fig. 1A).

Orientations were first examined in anaphase and telophase when the final cleavage plane has been established (Adams, 1996; Haydar et al., 2003; Sanada and Tsai, 2005). Most (82%) of the apically located cells divided vertically in WT cortices, 11% divided obliquely and 7% divided horizontally (Fig. 1B,D). By contrast, only 47% of cells in the cerebral cortex of Pax6$^{Sey/Sey}$ mutant mice divided with vertical cleavage planes, whereas oblique and horizontal angles were significantly increased reaching 25% and 28% of the cells, respectively (Fig. 1C,E) (see also Estivill-Torrus et al., 2002). We noticed that this difference in spindle orientation was already evident in metaphase cells (Fig. 1F,G), implying that the spindle orientation is altered prior to chromosome segregation in the Pax6$^{Sey/Sey}$ cerebral cortex. Notably, this difference in cleavage angles was not yet present at E12 when a similar proportion of mitotic cells divided with a non-vertical cleavage plane (25% WT, $n$=16 cells; 16% Pax6$^{Sey/Sey}$, $n$=19 cells). However, the profound increase in non-vertical divisions in Pax6$^{Sey/Sey}$ cerebral cortex persisted from E14 to E16 (non-vertical divisions: 30% WT, $n$=20 cells; 56% Pax6$^{Sey/Sey}$, $n$=41 cells). Taken together, these results show that Pax6 disruption alters the spindle orientation and cleavage plane in apical progenitors of the cerebral cortex starting at mid-neurogenesis.

## Unequal inheritance of adherens junction and apical membrane components is increased in the Pax6$^{Sey/Sey}$ cerebral cortex

To clarify whether these alterations in the cleavage plane result in alterations of the apical membrane partitioning, we examined cell division via en face confocal live imaging (see schematic in Fig. 2A). This permits unambiguous assignment of apical membrane domain inheritance by direct observation from the apical side in a whole-mount preparation. To do this, we electroporated pCAG-PACT-mKO1 and pCAG-ZO-1-GFP plasmids to monitor simultaneously the centrosome (PACT-mKO1, red fluorescence) and junctional component (ZO1-GFP, green fluorescence) as

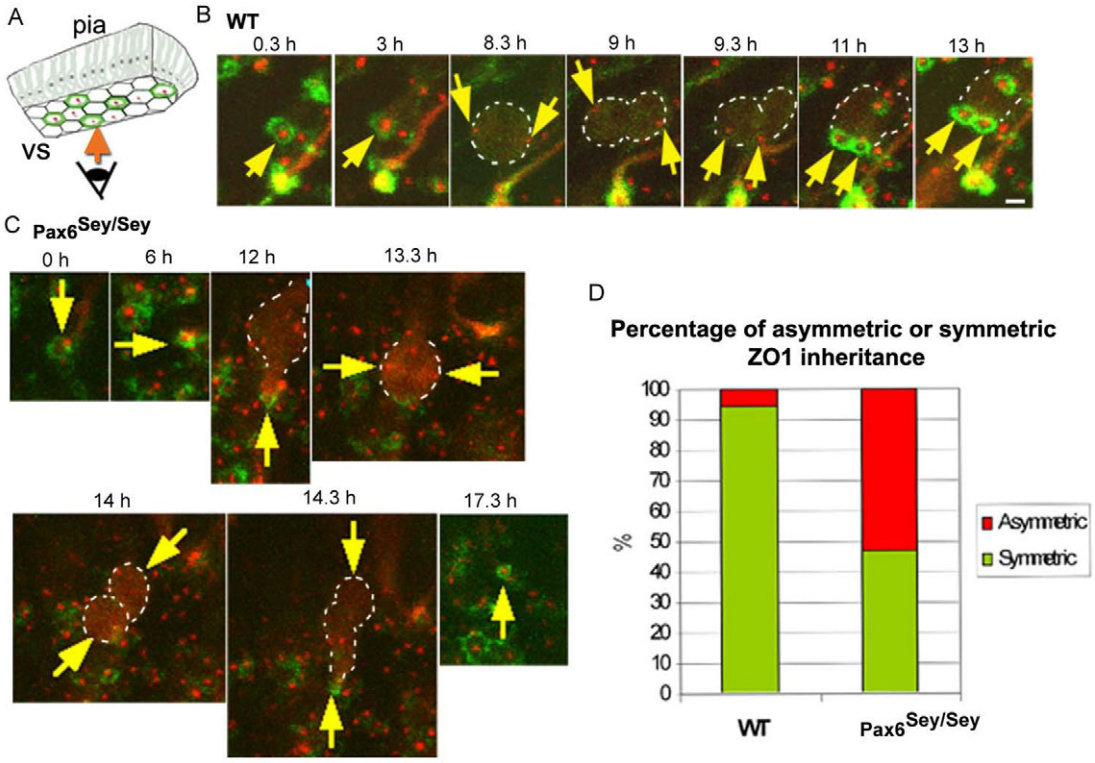


**Fig. 2. Increased cell divisions with asymmetric partitioning of the apical membrane in mouse Pax6$^{Sey/Sey}$ cerebral cortex.** (**A**) Schematic of en face imaging indicating the green EGFP-ZO1-marked cell boundaries and the red PACT-mKO1-labelled centrosomes at the ventricular surface (vs). (**B**,**C**) Yellow arrows depict red fluorescent centrosomes in micrographs from WT (B) and Pax6$^{Sey/Sey}$ mutant (C) cerebral cortex with low levels of cytoplasmic PACT-mKO1 delineating the cell body (white dashed line) at the times indicated at the top of each panel. B shows an example of symmetric division at the apical surface in WT cerebral cortex with the green ZO1 signal forming two rings after mitosis each containing a red centrosome (at 11 and 13 hours; for details, see supplementary material Movie 1), whereas C shows an example of asymmetric inheritance of the apical domain from Pax6$^{Sey/Sey}$ cerebral cortex with one daughter cell located relatively far from the apical surface (at 14 hours) without reforming a ZO1 ring at the apical surface. This division therefore resulted in a single ring of ZO1 enclosing a centrosome (at 17.3 hours), demonstrating that the apical membrane domain surrounded by the ZO1 ring was unequally inherited by the apical daughter cell. For details, see supplementary material Movie 2. (**D**) The mode of division shown in C occurred infrequently in WT but frequently in the Pax6$^{Sey/Sey}$ mutant as depicted in the histogram [18 (WT) and 16 (Pax6$^{Sey/Sey}$) divisions in more than two movies per genotype].

described previously (Konno et al., 2008). In these experiments, cell bodies located below the apical surface appear weakly red (see also Konno et al., 2008). In E14 WT cerebral cortex, labelled cell bodies occupied different positions according to their cell cycle stage, moving towards the apical surface during G2, consistent with the normal interkinetic nuclear migration of radial glial cells (supplementary material Movie 1). Amongst the observed apical mitoses, >90% generated daughters with near-identical ZO-1-GFP rings (Fig. 2B,D). In E14 Pax6$^{Sey/Sey}$ cerebral cortex, we observed a profound reduction in apical divisions with equal partitioning of the apical membrane to <50% (Fig. 2C,D; supplementary material Movie 2). Rather, the predominant apical division pattern in Pax6$^{Sey/Sey}$ mutant cells generated one daughter cell that did not inherit ZO1-GFP (Fig. 2C). Thus, live imaging not only confirmed the altered cell division angle in Pax6$^{Sey/Sey}$ cerebral cortex but revealed unambiguously that this results in a markedly unequal inheritance of the ZO1-labelled adherens junction components and the apical membrane domain enclosed by these.

In order to monitor the behaviour of the non-apical daughter cell, we also imaged slice preparations from E14 cerebral cortex after DiI labelling or electroporation of two GFP plasmids with cytoplasmic and membrane localization (supplementary material Movies 3-5). As illustrated in supplementary material Fig. S1, we observed many cell divisions in which one daughter cell lost its apical contact and moved basally, and the other daughter cell remained at the apical surface in slices of Pax6$^{Sey/Sey}$ cerebral cortex (e.g. cell indicated by red arrow in supplementary material Fig. S1A; see also supplementary material Movie 4). We also observed that the sub-apical daughter cell often did not migrate as far in the basal direction as those in WT and divided once again at the sub-apical position (11/17 randomly selected divisions; supplementary material Fig. S1B,C and Movie 5). Taken together, these data show that non-vertical cleavage angles in Pax6$^{Sey/Sey}$ cortex give rise to one, often still proliferative, daughter cell moving to a sub-apical position, thereby contributing to the increase in non-apical cell divisions.

## β-catenin and Par complex protein and mRNA levels are reduced in the Pax6$^{Sey/Sey}$ cerebral cortex

We asked next whether a decrease in Par proteins or other components of the adherens junctions (AJs) occurs in the absence of Pax6 function, possibly contributing to the alterations described above. aPKC (Fig. 3A) and Par3 (Fig. 3B-B″) immunostaining was very weak or undetectable at the apical surface of the Pax6$^{Sey/Sey}$ ventricular zone (VZ). A moderate decrease of N-cadherin

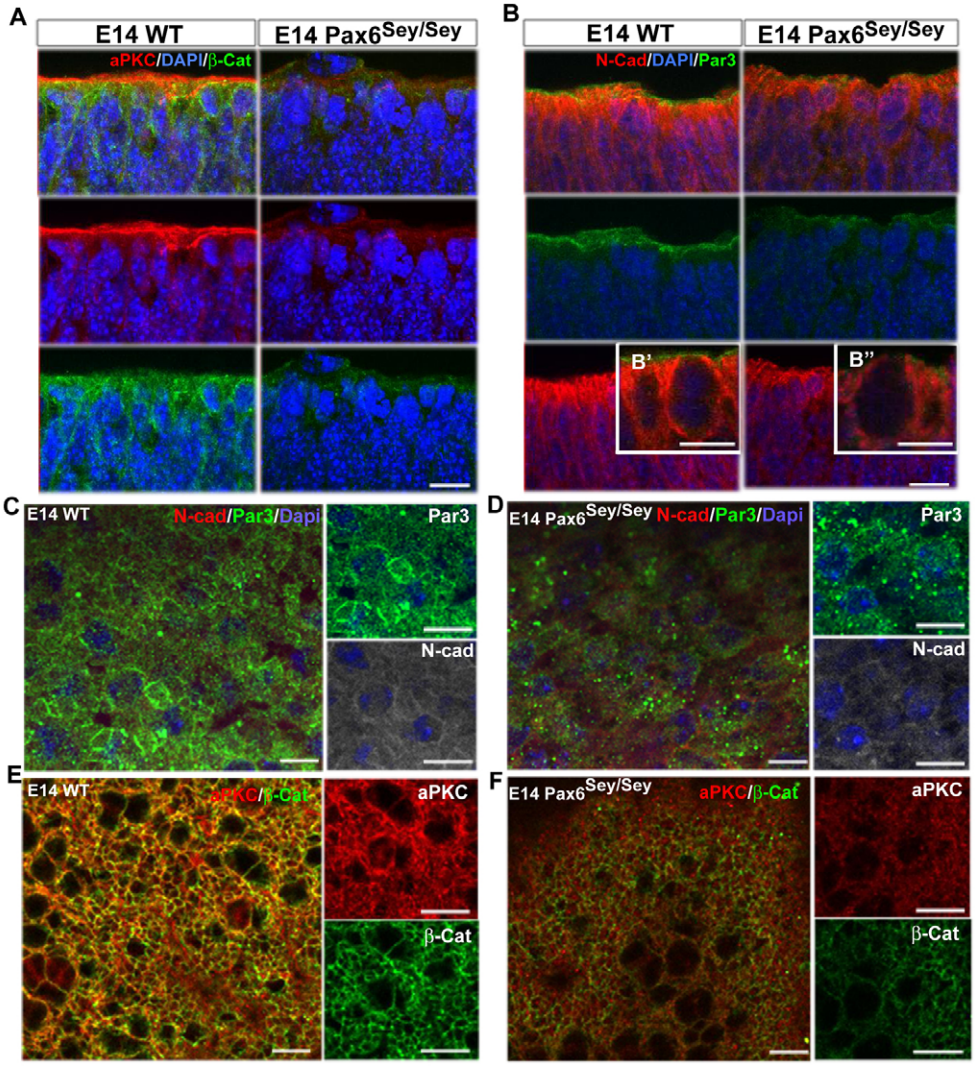


**Fig. 3. Decreased expression of adherens junction proteins in mouse Pax6$^{Sey/Sey}$ mutant cerebral cortices.** Fluorescence micrographs of coronal sections (**A**,**B**) or whole-mounts (**C-F**) viewed from the apical surface of WT and Pax6$^{Sey/Sey}$ cerebral cortices immunostained as indicated. B′ and B″ depict higher power views. A,B show *z*-stacked images and C-F show single confocal images. Scale bars: 10 μm in A,B; 5 μm in B′,B″; 10 μm in C-F.

immunostaining was observed in Pax6$^{Sey/Sey}$ versus WT cerebral cortex. This observation was confirmed in whole-mount preparations, indicating a profound reduction of Par3 (Fig. 3C,D), aPKC and β-catenin (AJ protein) (Fig. 3E,F) in Pax6$^{Sey/Sey}$ versus WT cerebral cortex. We also noted that the honeycomb structure of Par3 and aPKC immunopositive domains became indistinct, although β-catenin immunopositive domains were weaker but extant (Fig. 3C-F). Western blot analysis of cerebral cortex (supplementary material Fig. S2A) indicated that only the cytoplasmic pool of β-catenin was reduced in E14 Pax6$^{Sey/Sey}$ compared with WT, whereas no changes were visible between the nuclear fractions. Interestingly, qPCR analysis demonstrated a significant reduction of both β-*catenin* and *Pard3* (Par3) mRNA levels in E14 Pax6$^{Sey/Sey}$ to less than half of the levels in the WT cerebral cortex (supplementary material Fig. S2B). This reduction was also observed in apical progenitors isolated by FACS using prominin1 live immunostaining (data not shown). Given that Pax6 binding sites are present in the promoter regions of β-*catenin* and *Pard3* genes (supplementary material Fig. S2C), these data suggest that the decreased transcription levels are due to the lack of Pax6 function, thus contributing to the reduced protein levels. Thus, Pax6 might regulate several components of AJ coupling in order to maintain progenitors at the apical side.

## Non-apically dividing cells maintain the features of radial glia in the Pax6$^{Sey/Sey}$ cerebral cortex

Reduced levels of AJ coupling might result in premature delamination of apical progenitor cells, in which case one may expect that the delaminated progenitors retain hallmarks of the radial glial cells rather than maturing into basal progenitors (BPs). BPs are characterized by expression of the anti-proliferative neurogenic gene *Tis21* (*Btg2* – Mouse Genome Informatics), which is expressed in most BPs but only in a minor subpopulation of apical radial glial cells (Haubensak et al., 2004). BPs upregulate *Tis21* but downregulate radial glial hallmarks, such as BLBP (Fabp7 – Mouse Genome Informatics) or GLAST (Slc1a3 – Mouse Genome Informatics) (Pinto et al., 2009). Consistent with previous data (Haubensak et al., 2004), >80% of the basal mitoses immunostained for PH3 were GFP-positive in WT/*Tis21::GFP* cerebral cortices, whereas only 60% were GFP-positive in Pax6$^{Sey/Sey}$/*Tis21::GFP* littermates (Fig. 4A-D). The difference was even more pronounced with regard to GLAST, which was present in <5% of WT BPs, but was expressed in 65% of Pax6$^{Sey/Sey}$ basal mitotic cells (Fig. 4E). These data indicate that most of the basally dividing cells in the Pax6$^{Sey/Sey}$ cerebral cortex retain radial glia hallmarks consistent with their premature delamination.

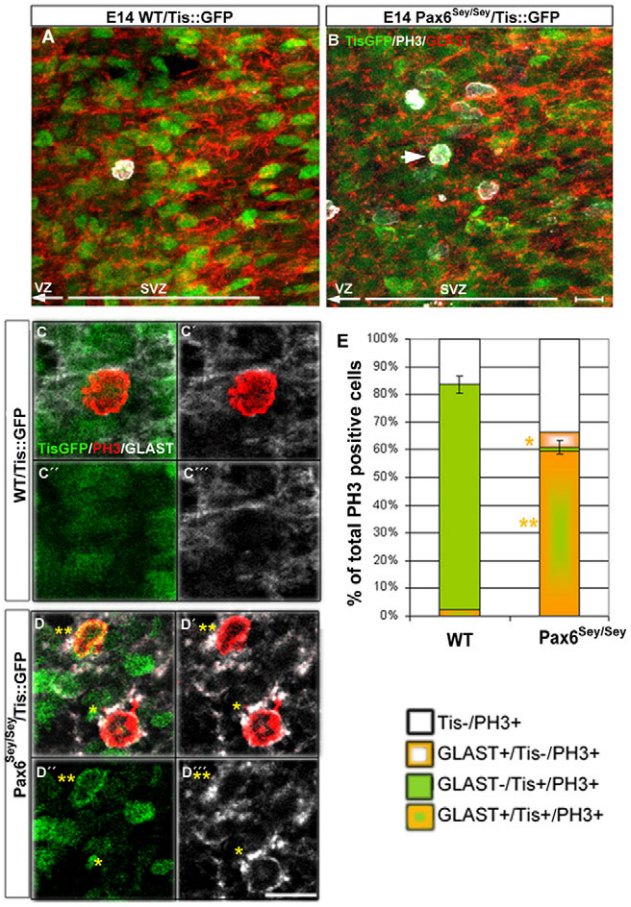


**Fig. 4. Basally dividing progenitors in mouse Pax6$^{Sey/Sey}$ cerebral cortex retain radial glia hallmarks.** (**A-D‴**) Fluorescence micrographs of the subventricular zone (SVZ) in coronal sections of the cerebral cortex from E14 WT/Tis21::GFP (A,C) and Pax6$^{Sey/Sey}$/Tis21::GFP mice (B,D) labelled as indicated. C-C‴,D-D‴ show single confocal sections. Single asterisk indicates a PH3+/GLAST+ cell and double asterisks a Tis+/PH3+/GLAST+ triple positive cell in D-D‴. (**E**) The proportion of PH3-positive basally dividing cells labelled for these markers as indicated by the colours (15 cells WT; 38 cells Pax6$^{Sey/Sey}$). Scale bars: 10 μm. Error bars represent s.e.m. *$P$<0.05, **$P$<0.005.

## De novo deletion of Pax6 alters the orientation of cell division and increases sub-apically dividing cells

As the experiments described above were performed in a mouse mutant with constitutive defects in Pax6-mediated transcription, the changes described above might have been indirectly elicited, e.g. as a result of the alterations in patterning (Stoykova et al., 1996; Stoykova et al., 2000; Toresson et al., 2000; Yun et al., 2001). To assess direct effects of Pax6, we acutely deleted it by electroporation of a plasmid containing Cre recombinase and GFP (Cre-PCIG) into the lateral ventricles of a conditional Pax6 mouse line in which exons 4-6 are flanked by *loxP* sites (Ashery-Padan et al., 2000). When GFP-positive cells were examined in the VZ 2 days after electroporation into WT or *Pax6$^{flox/flox}$* E12 embryos, i.e. at E14, Pax6 had been successfully deleted as Pax6-immunoreactive cells were reduced by >80% in *Pax6$^{flox/flox}$* compared with WT (Fig. 5A-C). We also observed downstream effects, including a decrease in the Pax6 target Ngn2 (Neurog2 – Mouse Genome Informatics), but not Tbr2 (Eomes – Mouse Genome Informatics), and a converse increase in Mash1 (Ascl1 – Mouse Genome Informatics) and Gsx2 (Fig. 5D,E; data not shown). Most importantly, within this short time window after elimination of Pax6 protein, the number of PH3-positive cells dividing sub-apically was already increased relative to electroporated cells in WT cortices (Fig. 5F,G). In addition, the orientation of apically dividing cells shifted towards non-vertical orientations upon Pax6 deletion (19% horizontal, 27% oblique, 54% vertical; $n$=41 cells), whereas most (95%) Cre-electroporated cells in control embryos divided with a vertical angle ($n$=19 cells; Fig. 5H,I). We also detected a moderate decrease in the gene expression levels of β-*catenin* and *Pard3* two days after Pax6 deletion (supplementary material Fig. S3A), which had not yet translated into decreased protein levels (supplementary material Fig. S3B).

## Lineage tracking of dissociated cells in vitro reveals effects of Pax6 on the mode of cell division

The experiments described above showed a rapid effect of Pax6 deletion on the orientation of cell division and increased generation of basally dividing progenitors, but could not determine to what extent these effects were due to alterations in cell polarity. We therefore asked whether alterations in the mode of cell division of Pax6$^{Sey/Sey}$ cerebral cortex cells were also present in a culture system independent of AJ coupling and apicobasal polarity. To this end, cells from cerebral cortices were dissociated and plated at densities at which most lacked cell-cell contacts during the first days of culture (Fig. 6A,B). Single-cell tracking by continuous live imaging (Costa et al., 2008) was then used to determine the mode of cell division by assessing the fate of the daughter cells. If both daughter cells proliferated again we referred to these as symmetric proliferative (SP) divisions; if both daughter cells did not divide for several days thereafter these were defined as symmetric terminal (ST) divisions; and an unequal behaviour with only one daughter cell dividing was designated an asymmetric (AS) division. Examples of such lineages are depicted in Fig. 6C. Consistent with our previous work, most (68%) cell divisions were SP and only a minority (12%) divided in an AS manner when cells had been isolated from E14 WT cerebral cortices (Fig. 6D). Conversely, many more cells isolated from Pax6$^{Sey/Sey}$ cortices generated asymmetric daughter cell fates (Fig. 6D). Thus, even under dissociated cell culture conditions, Pax6-mutant cells exhibit alterations in the mode of cell division.

The increased number of proliferating cells seen in the Pax6$^{Sey/Sey}$ cerebral cortex (Fig. 4A,B) (Haubst et al., 2004), is also maintained in this culture system with many more clones derived from Pax6$^{Sey/Sey}$ cerebral cortex cells containing PH3+ cells in mitoses (59%, $n$=81 clones) compared with those derived from WT cells (6%, $n$=31 clones) at 2 days in vitro. Thus, the impression that the increase in AS divisions occurs at the expense of SP divisions (Fig. 6D) is misleading, as SP divisions are only reduced in relative, but not in absolute numbers. Conversely, AS divisions are substantially increased among Pax6$^{Sey/Sey}$ cerebral cortex cells. This increase in AS divisions is not due to alterations in cell-cycle length (Fig. 6E) as is also the case in vivo (Quinn et al., 2007), demonstrating that alterations in the mode of cell division of Pax6$^{Sey/Sey}$ cells also occur independently of apicobasal polarity and AJ coupling.

To eliminate the possibility that the alterations observed in vitro, e.g. the increase in AS divisions, are due to an altered composition in progenitors, we isolated apical progenitor cells by FACS for prominin1, which is localized on the apical membrane of cortical

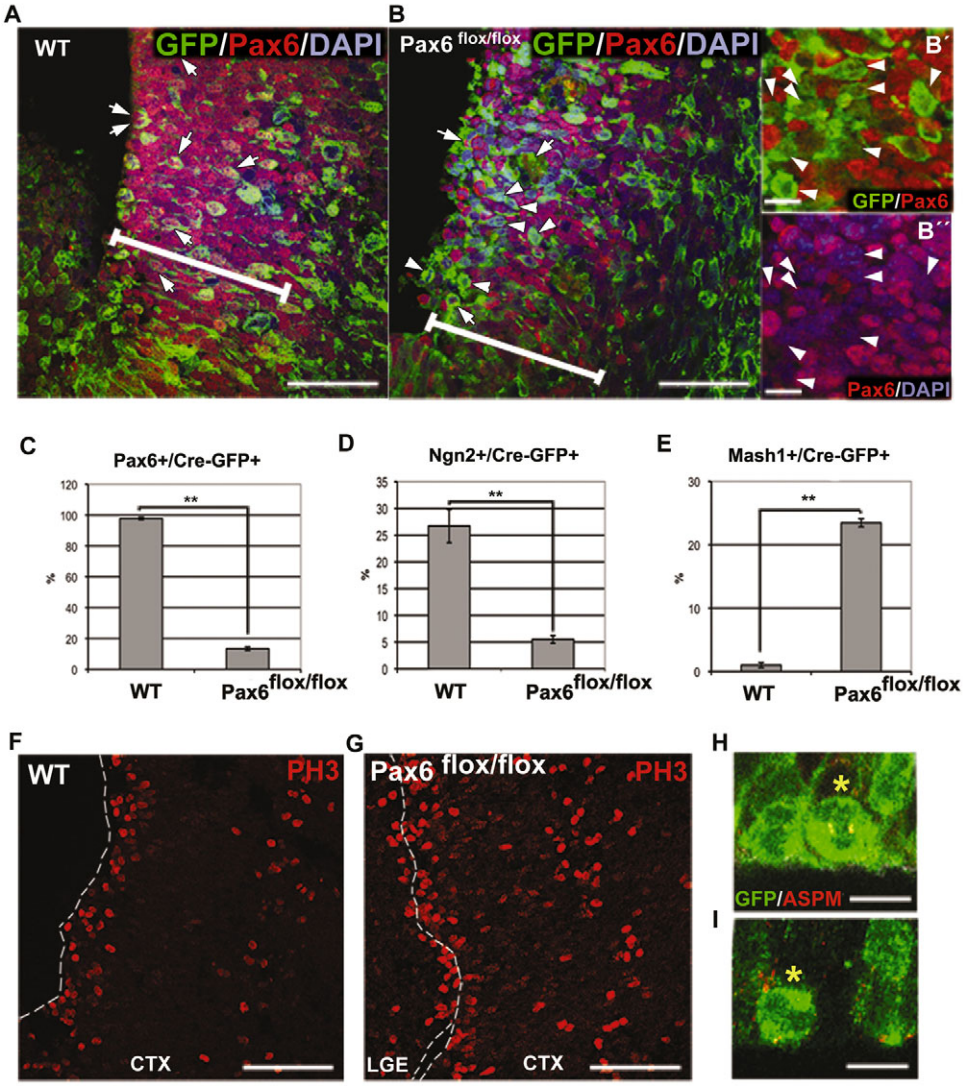


**Fig. 5. Increased basal divisions upon acute Pax6 deletion in mouse E14 cerebral cortex.** (**A-B″,F-I**) Micrographs depicting coronal sections of E14 WT (A,F,H) and Pax6$^{flox/flox}$ (B,G,I) cerebral cortices 2 days after electroporation with Cre-IRES-GFP plasmids immunolabelled as indicated. Arrows, Cre-GFP+, Pax6+ double-positive cells; arrowheads, Cre-GFP+, Pax6– cells (A,B). B′,B″ show higher magnification of Pax6-negative Cre-GFP+ cells from Pax6$^{flox/flox}$. Cre-GFP positive cell in metaphase is marked by an asterisk showing vertical cleavage angle in WT (H) and non-vertical cleavage angle in Pax6$^{flox/flox}$ (I). Dashed line in F,G indicates the ventricular surface of CTX. (**C-E**) The proportion of immunopositive cells quantified in the region indicated by the white bar in A,B (~100 μm distance from ventricular surface). Numbers of cells analyzed were: in WT brains, 351 (C), 162 (D), 224 (E); in Pax6$^{flox/flox}$ brains, 239 (C), 253 (D), 508 (E). Error bars represent s.e.m. $^{**}P<0.005$. Scale bars: 50 μm in A,B,F,G; 10 μm in B′,B″,H,I.

progenitors (Weigmann et al., 1997; Pinto et al., 2008) (supplementary material Fig. S4A,B). As expected, most of the isolated prominin1-positive cells (96%, *n*=22 trees) continued to proliferate in vitro (supplementary material Movie 6) exhibiting all three types of cell division (data not shown), whereas only 30% of prominin1-negative cells continued to divide (*n*=14 trees), consistent with this fraction comprising many differentiated neurons. Moreover, none of the prominin1-negative cells divided in an SP manner; rather, most (75%) divided in an ST manner, with the two daughters acquiring neuronal morphology (supplementary material Movie 7). This supports the notion that these prominin1-negative progenitors correspond to BPs that predominantly divide with an ST mode also in vivo (Haubensak et al., 2004; Miyata et al., 2004; Noctor et al., 2004; Wu et al., 2005; Attardo et al., 2008).

Cells derived from Pax6$^{Sey/Sey}$ cerebral cortices revealed remarkably different behaviour between prominin1-positive and -negative subpopulations (supplementary material Movies 8, 9): prominin1-positive Pax6$^{Sey/Sey}$ cells contained a higher proportion of non-dividing cells (20%), and amongst those continuing to divide (*n*=16 trees), 31% underwent AS divisions, an almost twofold increase compared with WT cells. The prominin1-negative fraction from Pax6$^{Sey/Sey}$ cortex, comprising the daughter cells losing the apical membrane domain observed in the en face imaging described above, also showed altered behaviour. Consistent with a decreased number of postmitotic neurons in the Pax6$^{Sey/Sey}$ cortex (Heins et al., 2002; Haubst et al., 2004), a larger fraction of prominin1-negative cells proliferated instead of generating two postmitotic neurons (supplementary material Movie 9). Like prominin1-negative cells isolated from WT, none of those from Pax6$^{Sey/Sey}$ cortex divided in an AS manner, further supporting the notion that increased AS division in the bulk cerebral cortex (Fig. 6D) was due to alterations in apical Pax6$^{Sey/Sey}$ mutant progenitors. Most strikingly, however, 40% of all cell divisions of the prominin1-negative fraction from the Pax6$^{Sey/Sey}$ cortex divided in a SP manner, which in WT is restricted to prominin1-positive apical progenitors.

Finally, we asked whether the increase in AS division amongst Pax6$^{Sey/Sey}$ cells is cell-autonomous using co-cultures of E14 WT cells at 100× excess with Pax6$^{Sey/Sey}$ cells crossed with a ubiquitously YFP-expressing mouse line (YVI) (George et al., 2007). Age-matched cells from WT/YVI mice (WT for the *Pax6* allele) served as controls. Also in this case, we observed increased numbers of AS divisions amongst progenitor cells from the Pax6$^{Sey/Sey}$ mutant in the first divisions but not in the second divisions (Fig. 6F; see tree

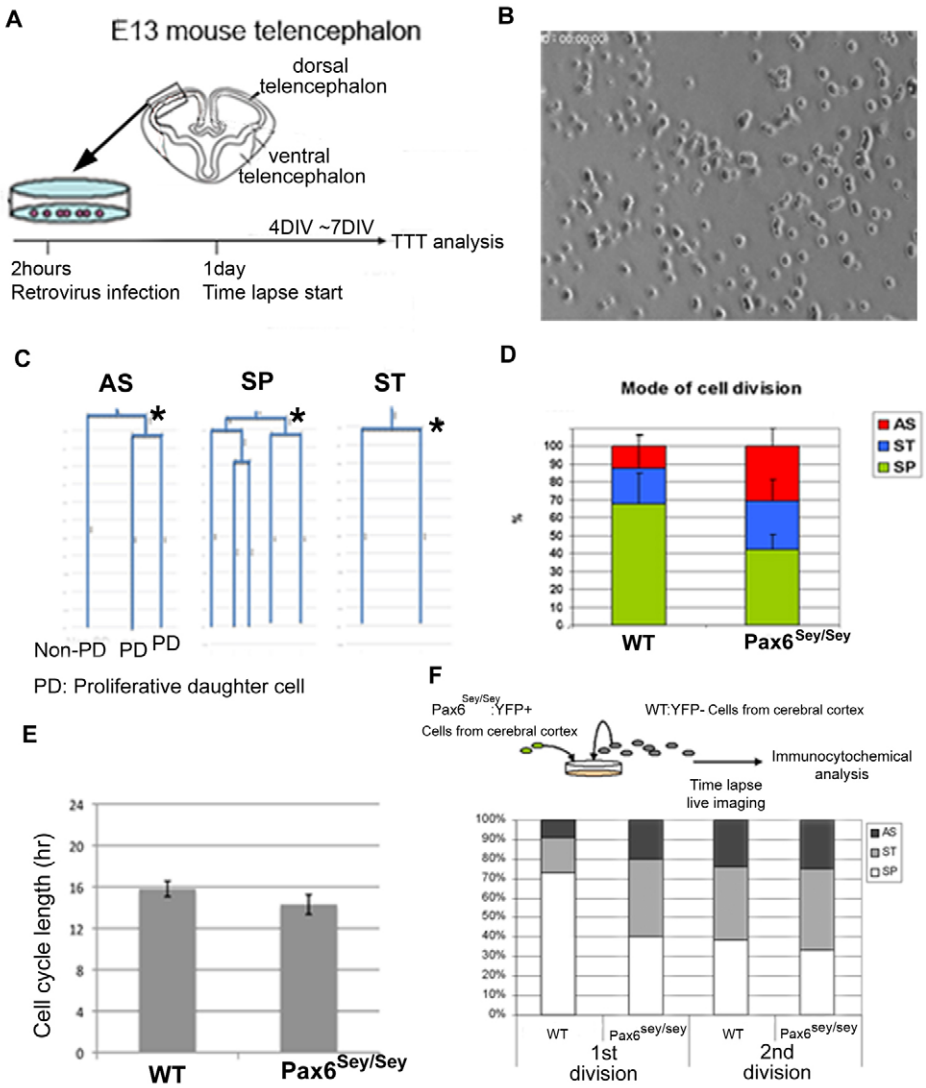


**Fig. 6. In vitro time lapse lineage tree analysis reveals increased asymmetric divisions in mouse Pax6$^{Sey/Sey}$ cerebral cortex cells.** (**A**) Schematic of the experimental paradigm. TTT, TTT tracking software. (**B**) Phase contrast image of the cell density at the start of the imaging. (**C**,**D**) Examples (indicated by asterisks) of asymmetric cell division (AS), symmetric proliferative division (SP) and symmetric terminal division (ST) in representative lineage trees quantified in D. Numbers of analyzed trees: 62 (WT), 75 (Pax6$^{Sey/Sey}$). (**E**,**F**) Cell cycle length in hours (hr) measured between the first and second division (E) and the proportion of the respective mode of cell division of YFP+ WT or Pax6$^{Sey/Sey}$ cells co-cultured with WT cells (F). Numbers of analyzed trees: 11 (WT), 15 (Pax6$^{Sey/Sey}$). Error bars represent s.e.m. 1st divisions and 2nd divisions correspond to the mode at single asterisk or double asterisks in supplementary material Fig. S4C, respectively.

examples in supplementary material Fig. S4C). This indicates that the increase in AS cell divisions amongst Pax6$^{Sey/Sey}$ progenitors is likely to be caused by cell-intrinsic mechanisms.

## *Spag5* is a direct target of Pax6 and regulates the orientation of cell division

Given that the cell-autonomous alterations in the cell division mode are independent of apicobasal polarity, we next asked whether Pax6 directly affects the machinery regulating the mode of cell division. We searched the available transcriptome and ChIP data of Pax6 in cerebral cortex and lens (Holm et al., 2007; Sansom et al., 2009; Wolf et al., 2009) to identify possible target genes of Pax6 that might affect cell division. One candidate was the sperm associated antigen 5 (Spag5 or mAstrin), a microtubule-associated protein (Thein et al., 2007; Cheng et al., 2007) localizing to spindle poles and kinetochores in mammalian cells (Mack and Compton, 2001). Consistent with a possible regulation by Pax6, *Spag5* mRNA levels were already reduced in E12 Pax6$^{Sey/Sey}$ cerebral cortex compared with WT littermates (Fig. 7A). Surprisingly, however, mRNA as well as protein levels increased at later stages (Fig. 7A and supplementary material Fig. S5A). In the context of the specific recruitment of Spag5 only to kinetochores of chromosomes in the metaphase plate (Manning et al., 2010), it is of interest that the intensity of Spag5 immunoreactivity in cultured Pax6$^{Sey/Sey}$ cells was affected in prometaphase and metaphase, but not in anaphase, even though Spag5 immunoreactivity was also observed at other locations in the cytoplasm (supplementary material Fig. S5B,C). Given the initial reduction and later increase in *Spag5* mRNA levels in Pax6$^{Sey/Sey}$ mutant, we examined *Spag5* mRNA levels upon de novo elimination of Pax6 by Cre electroporation (supplementary material Fig. S3). Similar to the reduction of *Spag5* mRNA levels in the Pax6$^{Sey/Sey}$ mutant cortex at early developmental time points, acute deletion of Pax6 also caused a reduction in *Spag5* mRNA levels (supplementary material Fig. S3A). As these data were consistent with a direct regulation of *Spag5* by Pax6, we used Genomatix software analysis to assess possible Pax6 binding sites in the *Spag5* promoter region (Fig. 7B) and validated its direct regulation by Pax6 in two independent assays. First, Pax6 transduction positively regulated a luciferase construct containing the *Spag5* promoter region with the Pax6 binding site (Fig. 7C). Second, ChIP with a Pax6 antibody revealed substantial enrichments of *Spag5* promoter regions ~1 kb upstream and downstream of the *Spag5* translational start codon [–1 and +1 ($P$<0.001) and +2 ($P$<0.01)] confirming Pax6 binding at these sites (Fig. 7D). Thus, *Spag5* is directly regulated by Pax6 in cortical progenitor cells. In order to determine its role in these progenitor

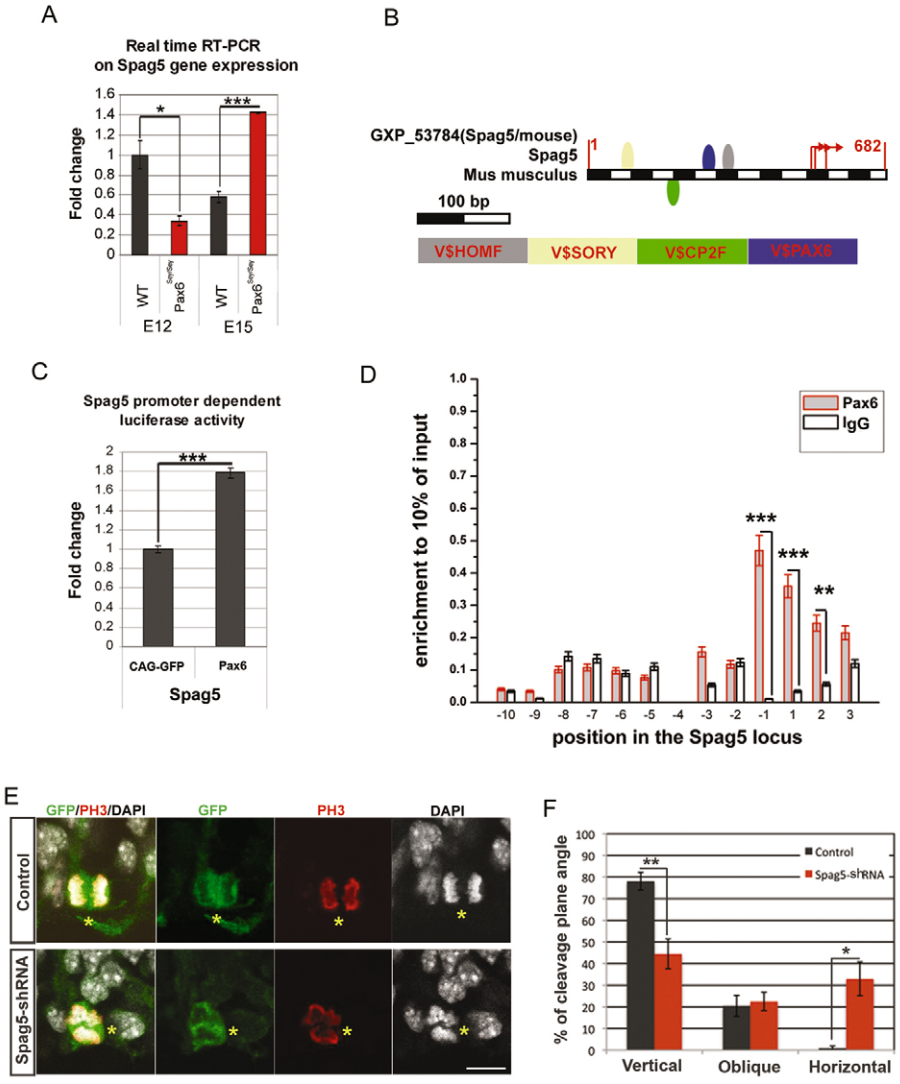


**Fig. 7. Direct interaction between Pax6 and *Spag5* promoter region.** (**A**) mRNA (triplicates of three different biological replicates per genotype) levels of *Spag5* at E12 and E15. (**B**) Schematic of the mouse *Spag5* gene promoter. Putative Pax6 binding sites are represented by the blue box (Gene2Promoter; Genomatix and FrameWorker). (**C**) The *Spag5*-promoter luciferase construct was co-transduced into HEK293 cells either with Pax6-pCAG or control (pCAG) together with 0.1 μg of the pRL-TK plasmid encoding *Renilla* luciferase. Results are expressed as mean ± s.e.m. of the ratio between *Renilla* luciferase and firefly (control) luciferase activities. (**D**) Pax6 distribution at the mouse *Spag5* gene locus in cerebral cortex chromatin. The numbers on the *x*-axis represent the primer position (~13 kb around ATG) in the *Spag5* locus. The primer position 1 corresponds to ATG of the *Spag5* gene. An anti-IgG immunoprecipitation was performed as a negative control for each primer set. The relative enrichment unit represents 10% of the input. (**E**) E12 cerebral cortices were electroporated with pSuper.gfp/neo-Spag5 or pSuper.gfp/neo and labelled for anti-GFP and anti-PH3 at E14 together with DAPI counter staining. Micrographs depict exemplified pictures of GFP-positive apically dividing cells (indicated by asterisks). Cells with vertical cleavage angle from control (upper panels) or with non-vertical cleavage angle from *Spag5*-shRNA (lower panels) plasmid-electroporated cerebral cortices, respectively, are shown. (**F**) *Spag5*-shRNA-induced alteration of cleavage plane angle amongst apically dividing cells [control: *n*=3 animals (64 cells), *Spag5*-shRNA: *n*=4 animals (78 cells)]. Cleavage plane angle of GFP-positive apically dividing cells was analyzed and classified as described in Fig. 1. Data represent the mean ± s.e.m. **P*<0.05, ***P*<0.01, ****P*<0.001. Scale bar: 10 μm.

cells, we constructed a shRNA vector against *Spag5* and electroporated it into E12 WT cerebral cortices. Notably, this led to a significant increase in non-vertical cleavage planes of apical progenitors compared with cells electroporated with the control vector two days later (E14, Fig. 7E,F), consistent with a role of Spag5 in spindle organization in other cell types (Yuan et al., 2009). Taken together, these data strongly support the concept that Pax6 directly regulates target genes involved in regulating the mode of cell division.

## DISCUSSION

Here, we report a novel function for Pax6: namely, its role in regulating the orientation and mode of cell division. We first demonstrated by spindle pole staining that the cleavage plane angle was altered in radial glial cells of $Pax6^{Sey/Sey}$ cerebral cortex starting at mid-neurogenesis. This was confirmed by live imaging in en face preparations, revealing a marked increase in divisions with unequal inheritance of the apical membrane domain in $Pax6^{Sey/Sey}$ cerebral cortex. Acute deletion of Pax6 also lead to

increased non-vertical divisions amongst apical progenitors and an increase in non-apical cell divisions. Finally, we demonstrated an increase in cell divisions with asymmetric daughter cell fates in dissociated cell cultures independent of apicobasal polarity. From these data, we conclude that Pax6 affects cortical progenitor cell division on at least three levels: by weakening the anchoring of apical progenitors, by altering the cleavage plane of apical progenitors and by apicobasal polarity-independent mechanisms.

## Pax6 regulates adhesion and apical anchoring of apical progenitors

The increase in non-apically dividing progenitors in the Pax6$^{Sey/Sey}$ cerebral cortex has long been known (Götz et al., 1998), but the different mechanisms contributing to it are only now being elucidated. Impaired interkinetic nuclear migration of radial glial cells, as observed in the rat Pax6$^{Sey/Sey}$ (Tamai et al., 2007) and confirmed in our imaging analysis in the mouse Pax6$^{Sey/Sey}$, causes a subset of cells to undergo cell division prior to reaching the ventricular surface. We demonstrated in this work two additional mechanisms contributing to this phenotype: an increase in delamination of apical progenitors and an increase in apical progenitors dividing with non-vertical orientation to generate one daughter cell devoid of apical membrane and anchoring. Increased apical progenitor cell delamination would be facilitated by the profound decrease in molecules anchoring neuroepithelial and radial glial cells at the ventricular surface in the Pax6$^{Sey/Sey}$ cerebral cortex, such as R-cadherin (Stoykova et al., 1997), β-catenin and members of the Par complex, as shown here. These molecules are all likely to anchor apical progenitors from their function in adherens junction complexes (Cappello et al., 2006; Costa et al., 2008; Bultje et al., 2009; Fumalski et al., 2010; Machon et al., 2003; Woodhead et al., 2006; Zhang et al., 2010); these (supplementary material Fig. S2) and other proteins regulating cell adhesion, such as *Shroom3* and *Olfm3* (optimedin), have been identified as direct Pax6 targets (Plageman et al., 2010; Grinchuk et al., 2005; Sansom et al., 2009). Thus, Pax6 appears to influence AJ coupling and apical anchoring via functionally related target gene regulation.

## Pax6 regulates the orientation of cell division via transcriptional regulation of *Spag5*

Alterations in AJ coupling might not only affect anchoring of cells but also spindle orientation, as spindle poles are aligned with junctional complexes in many epithelial cell divisions exhibiting a vertical cleavage angle (Lechler and Fuchs, 2005; Poulson and Lechler, 2010; Zheng et al., 2010). In this regard, the novel Pax6 target gene we describe here, *Spag5*, is of particular interest as its product has been shown to associate with the mitotic spindle and the centrosome, and regulates aurora A (aurora kinase A – Mouse Genome Informatics) localization in mammalian cell division (Chang et al., 2001; Mack and Compton, 2001; Cheng et al., 2007; Du et al., 2008; Yuan et al., 2009). Pax6 regulates the transcription of *Spag5*, as shown here by expression analysis after acute Pax6 deletion, luciferase assays and ChIP, and Spag5 knockdown phenocopies the increase in non-vertical cell divisions as observed in the Pax6-deficient cerebral cortex, both in Pax6$^{Sey/Sey}$ mice or after acute Pax6 depletion by Cre electroporation. Spag5 is associated with the spindle machinery in other cell types and is implicated in regulating kinetochore microtubule dynamics (Manning et al., 2010) and interacts with spindle-associated proteins, such as aurora A (Du et al., 2008) and ninein (Cheng et al., 2007). Ninein is also a Pax6 target regulating centrosomal microtubule nucleation and asymmetric inheritance of the mother centrosome in cerebral cortex progenitor cells (Wang et al., 2009). Indeed, ninein expression levels were also affected in the E15 Pax6$^{Sey/Sey}$ cerebral cortex (supplementary material Fig. S5D), suggesting complex quantitative alterations in proteins associated with centrosome and microtubule function in the absence of Pax6. Taken together, our data suggest the direct regulation of proteins associated with the spindle machinery by Pax6-mediated transcription.

As knockdown of Spag5 increased non-vertical cell division in WT cerebral cortex, these data also demonstrate a role for Pax6 in regulating the orientation of cell division independently of other phenotypes observed in the Pax6$^{Sey/Sey}$ mutant cerebral cortex, such as alterations in patterning (Walther and Gruss, 1991; Stoykova and Gruss, 1994; Stoykova et al., 1996; Torresson et al., 2000; Yun et al., 2001). The extent to which these targets are also responsible for polarity-independent effects of Pax6 on the mode of cell division remains to be determined. Prominin1-expressing VZ progenitor cells from the Pax6$^{Sey/Sey}$ mutant showed an increase in the generation of daughter cells with asymmetric cell fates (postmitotic versus dividing), even in a culture system in which AJ coupling and apicobasal polarity were absent, or upon co-culturing with WT cells. This suggests that Pax6 regulates the mode of cell division independently of apicobasal polarity and AJ coupling. These data, therefore, highlight the importance of examining Pax6 target genes for a better understanding of transcriptional regulation of the mode of cell division.

## Phylogenetic relevance

Polarity is important not only for the mode of progenitor cell division, but also to regulate tangential or radial expansion of a given brain region. These mechanisms are of special importance with regard to expansion of the cerebral cortex in primate evolution. Radial glial cells lacking apical contact to the ventricular surface, so-called ‘outer radial glia’ (oRG), have recently been discovered in much larger numbers in ferret and primate cerebral cortex compared with that of mouse (Hansen et al., 2010; Fietz et al., 2010; Reillo et al., 2011). Notably, non-apical progenitor cell increases in Pax6$^{Sey/Sey}$ mutant (mouse) cerebral cortex have some similarities to oRG as they maintain radial glial hallmarks, such as the expression of GLAST, and an SP mode of cell division as observed by single cell tracking of prominin1-negative progenitors in dissociated cultures. This phenotype is also accompanied by reduced tangential expansion of the Pax6$^{Sey/Sey}$ cerebral cortex (supplementary material Fig. S6). It is, therefore, intriguing to speculate that alterations in the orientation of cell division and apical anchoring by AJ coupling might contribute to the generation of sub-apically dividing radial glia, thereby regulating tangential versus radial expansion of the cerebral cortex in ontogeny and phylogeny.

**Acknowledgements**

We are particularly grateful to Fumio Matsuzaki for providing us with plasmids pCAG-ZO1-EGFP and pCAG-PACT-mKO1 and great advice for establishing the en face imaging. We would like to thank Fumio Matsuzaki, Pia Johansson and Tony Perry for insightful comments on the manuscript as well as Tessa Walcher, Ingo Burtscher and Adam Filipczyk for technical advice in the course of this work. We greatly appreciate the excellent technical assistance of Andrea Steiner, Detlef Franzen, Timucin Öztürk and Angelika Waiser.

**Funding**

This work was supported by grants of the Bavarian State Ministry of the Sciences, Research and the Arts, Bundesministerium für Bildung und Forschung (BMBF), Deutsche Forschungsgemeinschaft (DFG), European Union (EU) and the Helmholtz Association to M.G. and DFG to T.S.

**Competing interests statement**
The authors declare no competing financial interests.

**Supplementary material**
Supplementary material available online at
http://dev.biologists.org/lookup/suppl/doi:10.1242/dev.074591/-/DC1

**References**

**Adams, R. J.** (1996). Metaphase spindles rotate in the neuroepithelium of rat cerebral cortex. *J. Neurosci.* **16**, 7610-7618.
**Alexandre, P., Reugels, A. M., Barker, D., Blanc, E. and Clarke J. D.** (2010). Neurons derive from the more apical daughter in asymmetric divisions in the zebrafish neural tube. *Nat. Neurosci.* **13**, 673-679.
**Ashery-Padan, R., Marquardt, T., Zhou, X. and Gruss, P.** (2000). Pax6 activity in the lens primordium is required for lens formation and for correct placement of a single retina in the eye. *Genes Dev.* **14**, 2701-2711.
**Attardo, A., Calegari, F., Haubensak, W., Wilsch-Brauninger, M. and Huttner, W. B.** (2008). Live imaging at the onset of cortical neurogenesis reveals differential appearance of the neuronal phenotype in apical versus basal progenitor progeny. *PLoS ONE* **3**, e2388.
**Berger, J., Berger, S., Tuoc, T. C., D'Amelio, M., Cecconi, F., Gorski, J. A., Jones, K. R., Gruss, P. and Stoykova, A.** (2007). Conditional activation of Pax6 in the developing cortex of transgenic mice causes progenitor apoptosis. *Development* **134**, 1311-1322.
**Bultje, R. S., Castaneda-Castellanos, D. R., Jan, L. Y., Jan, Y. N., Kriegstein, A. R. and Shi, S. H.** (2009). Mammalian Par3 regulates progenitor cell asymmetric division via notch signaling in the developing neocortex. *Neuron* **63**, 189-202.
**Cappello, S., Attardo, A., Wu, X., Iwasato, T., Itohara, S., Wilsch-Brauninger, M., Eilken, H. M., Rieger, M. A., Schroeder, T. T., Huttner, W. B. et al.** (2006). The Rho-GTPase cdc42 regulates neural progenitor fate at the apical surface. *Nat. Neurosci.* **9**, 1099-1107.
**Carey, M. F., Peterson, C. L. and Smale, S. T.** (2009). Chromatin immunoprecipitation (ChIP). *Cold Spring Harb. Protoc.* **9**, Prot5279.
**Chang, M. S., Huang, C. J., Chen, M. L., Chen, S. T., Fan, C. C., Chu, J. M., Lin, W. C. and Yang, Y. C.** (2001). Cloning and characterization of hMAP126, a new member of mitotic spindle-associated proteins. *Biochem. Biophys. Res. Commun.* **287**, 116-121.
**Cheng, T. S., Hsiao, Y. L., Lin, C. C., Hsu, C. M., Chang, M. S., Lee, C. I., Yu, R. C., Huang, C. Y., Howng, S. L. and Hong, Y. R.** (2007). hNinein is required for targeting spindle-associated protein Astrin to the centrosome during the S and G2 phases. *Exp. Cell Res.* **313**, 1710-1721.
**Chenn, A. and McConnell, S. K.** (1995). Cleavage orientation and the asymmetric inheritance of Notch1 immunoreactivity in mammalian neurogenesis. *Cell* **82**, 631-641.
**Costa, M. R., Wen, G., Lepier, A., Schroeder, T. and Gotz, M.** (2008). Par-complex proteins promote proliferative progenitor divisions in the developing mouse cerebral cortex. *Development* **135**, 11-22.
**Doe, C. Q.** (2008). Neural stem cells: balancing self-renewal with differentiation. *Development* **135**, 1575-1587.
**Du, J., Jablonski, S., Yen, T. J. and Hannon, G. J.** (2008). Astrin regulates Aurora-A localization. *Biochem. Biophys. Res. Commun.* **370**, 213-219.
**Estivill-Torrus, G., Pearson, H., van Heyningen, V., Price, D. J. and Rashbass, P.** (2002). Pax6 is required to regulate the cell cycle and the rate of progression from symmetrical to asymmetrical division in mammalian cortical progenitors. *Development* **129**, 455-466.
**Farkas, L. M. and Huttner, W. B.** (2008). The cell biology of neural stem and progenitor cells and its significance for their proliferation versus differentiation during mammalian brain development. *Curr. Opin. Cell Biol.* **20**, 707-715.
**Fietz, S. A., Kelava, I., Vogt, J., Wilsch-Brauninger, M., Stenzel, D., Fish, J. L., Corbeil, D., Riehn, A., Distler, W., Nitsch, R. et al.** (2010). OSVZ progenitors of human and ferret neocortex are epithelial-like and expand by integrin signaling. *Nat. Neurosci.* **13**, 690-699.
**Fish, J. L., Kosodo, Y., Enard, W., Paabo, S. and Huttner, W. B.** (2006). Aspm specifically maintains symmetric proliferative divisions of neuroepithelial cells. *Proc. Natl. Acad. Sci. USA* **103**, 10438-10443.
**Fish, J. L., Dehay, C., Kennedy, H. and Huttner, W. B.** (2008). Making bigger brains-the evolution of neural-progenitor-cell division. *J. Cell Sci.* **121**, 2783-2793.
**Fumalski, J. K., Trivedi, N., Howell, D., Yang, Y., Tong, Y., Gilbertson, R. and Solecki, D. J.** (2010). Siah regulation of Pard3A controls neuronal cell adhesion during germinal zone exit. *Science* **330**,1834.
**George, S. H., Gertsenstein, M., Vintersten, K., Korets-Smith, E., Murphy, J., Stevens, M. E., Haigh, J. J. and Nagy, A.** (2007). Developmental and adult phenotyping directly from mutant embryonic stem cells. *Proc. Natl. Acad. Sci. USA* **104**, 4455-4460.
**Godin, J. D., Colombo, K., Molina-Calavita, M., Keryer, G., Zala, D., Charrin, B. C., Dietrich, P., Volvert, M. L., Guillemot, F., Dragatsis, I. et al.** (2010). Huntingtin is required for mitotic spindle orientation and mammalian neurogenesis. *Neuron* **67**, 392-406.
**Götz, M. and Huttner, W. B.** (2005). The cell biology of neurogenesis. *Nat. Rev. Mol. Cell. Biol.* **6**, 777-788.
**Götz, M., Stoykova, A. and Gruss, P.** (1998). Pax6 controls radial glia differentiation in the cerebral cortex. *Neuron* **21**, 1031-1044.
**Grinchuk, O., Kozmik, Z., Wu, X. and Tomarev, S.** (2005). The Optimedin gene is a downstream target of Pax6. *J. Biol. Chem.* **280**, 35228-35237.
**Hand, R., Bortone, D., Mattar, P., Nguyen, L., Heng, J. I., Guerrier, S., Boutt, E., Peters, E., Barnes, A. P., Parras, C. et al.** (2005). Phosphorylation of Neurogenin2 specifies the migration properties and the dendritic morphology of pyramidal neurons in the neocortex. *Neuron* **48**, 45-62.
**Hansen, D. V., Lui, J. H., Parker, P. R. and Kriegstein, A. R.** (2010). Neurogenic radial glia in the outer subventricular zone of human neocortex. *Nature* **464**, 554-561.
**Haubensak, W., Attardo, A., Denk, W. and Huttner, W. B.** (2004). Neurons arise in the basal neuroepithelium of the early mammalian telencephalon: a major site of neurogenesis. *Proc. Natl. Acad. Sci. USA* **101**, 3196-3201.
**Haubst, N., Berger, J., Radjendirane, V., Graw, J., Favor, J., Saunders, G. F., Stoykova, A. and Gotz, M.** (2004). Molecular dissection of Pax6 function: the specific roles of the paired domain and homeodomain in brain development. *Development* **131**, 6131-6140.
**Haydar, T. F., Ang, E., Jr and Rakic, P.** (2003). Mitotic spindle rotation and mode of cell division in the developing telencephalon. *Proc. Natl. Acad. Sci. USA* **100**, 2890-2895.
**Heins, N., Malatesta, P., Cecconi, F., Nakafuku, M., Tucker, K. L., Hack, M. A., Chapouton, P., Barde, Y. A. and Götz, M.** (2002). Glial cells generate neurons: the role of the transcription factor Pax6. *Nat. Neurosci.* **5**, 308-315.
**Hill, R. E., Favor, J., Hogan, B. L., Ton, C. C., Saunders, G. F., Hanson, I. M., Prosser, J., Jordan, T., Hastie, N. D. and van Heyningen, V.** (1991). Mouse small eye results from mutations in a paired-like homeobox-containing gene. *Nature* **354**, 522-525.
**Holm, P. C., Mader, M. T., Haubst, N., Wizenmann, A., Sigvardsson, M. and Götz, M.** (2007). Loss- and gain-of-function analyses reveal targets of Pax6 in the developing mouse telencephalon. *Mol. Cell. Neurosci.* **34**, 99-119.
**Huttner, W. B. and Kosodo, Y.** (2005). Symmetric versus asymmetric cell division during neurogenesis in the developing vertebrate central nervous system. *Curr. Opin. Cell Biol.* **17**, 648-657.
**Knoblich, J. A.** (2008). Mechanisms of asymmetric stem cell division. *Cell* **132**, 583-597.
**Konno, D., Shioi, G., Shitamukai, A., Mori, A., Kiyonari, H., Miyata, T. and Matsuzaki, F.** (2008). Neuroepithelial progenitors undergo LGN-dependent planar divisions to maintain self-renewability during mammalian neurogenesis. *Nat. Cell Biol.* **10**, 93-101.
**Kosodo, Y., Roper, K., Haubensak, W., Marzesco, A. M., Corbeil, D. and Huttner, W. B.** (2004). Asymmetric distribution of the apical plasma membrane during neurogenic divisions of mammalian neuroepithelial cells. *EMBO J.* **23**, 2314-2324.
**Kriegstein, A., Noctor, S. and Martinez-Cerdeno, V.** (2006). Patterns of neural stem and progenitor cell division may underlie evolutionary cortical expansion. *Nat. Rev. Neurosci.* **7**, 883-890.
**Lechler, T. and Fuchs, E.** (2005). Asymmetric cell divisions promote stratification and differentiation of mammalian skin. *Nature* **437**, 275-280.
**Lee, T. I., Johnstone, S. E. and Young, R. A.** (2006). Chromatin immunoprecipitation and microarray-based analysis of protein location. *Nat. Protoc.* **1**, 729-748.
**Machon, O., van den Bout, C. J., Backman, M., Kemler, R. and Krauss, S.** (2003). Role of beta-catenin in the developing cortical and hippocampal neuroepithelium. *Neuroscience* **122**, 129-143.
**Mack, G. J. and Compton, D. A.** (2001). Analysis of mitotic microtubule-associated proteins using mass spectrometry identifies astrin, a spindle-associated protein. *Proc. Natl. Acad. Sci. USA* **98**, 14434-14439.
**Manning, A. L., Bakhoum, S. F., Maffini, S., Correia-Melo, C., Maiato, H. and Compton, D. A.** (2010). CLASP1, astrin and Kif2b form a molecular switch that regulates kinetochore-microtubule dynamics to promote mitotic progression and fidelity. *EMBO J.* **29**, 3531-3543.
**Marthiens, V. and ffrench-Constant, C.** (2009). Adherens junction domains are split by asymmetric division of embryonic neural stem cells. *EMBO Rep.* **10**, 515-520.
**Matsuzaki, F.** (2000). Asymmetric division of *Drosophila* neural stem cells: a basis for neural diversity. *Curr. Opin. Neurobiol.* **10**, 38-44.
**Miyata, T.** (2007). Asymmetric cell division during brain morphogenesis. *Prog. Mol. Subcell. Biol.* **45**, 121-142.
**Miyata, T., Kawaguchi, A., Saito, K., Kawano, M., Muto, T. and Ogawa, M.** (2004). Asymmetric production of surface-dividing and non-surface-dividing cortical progenitor cells. *Development* **131**, 3133-3145.
**Molnar, Z., Metin, C., Stoykova, A., Tarabykin, V., Price, D. J., Francis, F., Meyer, G., Dehay, C. and Kennedy, H.** (2006). Comparative aspects of cerebral cortical development. *Eur. J. Neurosci.* **23**, 921-934.
**Morin, X., Jaouen, F. and Durbec, P.** (2007). Control of planar divisions by the G-protein regulator LGN maintains progenitors in the chick neuroepithelium. *Nat. Neurosci.* **10**, 1440-1448.

**Ninkovic, J., Pinto, L., Petricca, S., Lepier, A., Sun, J., Rieger, M. A., Schroeder, T., Cvekl, A., Favor, J. and Gotz, M.** (2010). The transcription factor Pax6 regulates survival of dopaminergic olfactory bulb neurons via crystallin alphaA. *Neuron* **68**, 682-694.
**Noctor, S. C., Martinez-Cerdeno, V., Ivic, L. and Kriegstein, A. R.** (2004). Cortical neurons arise in symmetric and asymmetric division zones and migrate through specific phases. *Nat. Neurosci.* **7**, 136-144.
**Osumi, N.** (2001). The role of Pax6 in brain patterning. *Tohoku J. Exp. Med.* **193**, 163-174.
**Osumi, N., Shinohara, H., Numayama-Tsuruta, K. and Maekawa, M.** (2008). Concise review: Pax6 transcription factor contributes to both embryonic and adult neurogenesis as a multifunctional regulator. *Stem Cells* **26**, 1663-1672.
**Pinto, L., Mader, M. T., Irmler, M., Gentilini, M., Santoni, F., Drechsel, D., Blum, R., Stahl, R., Bulfone, A., Malatesta, P. et al.** (2008). Prospective isolation of functionally distinct radial glial subtypes-lineage and transcriptome analysis. *Mol. Cell. Neurosci.* **38**, 15-42.
**Pinto, L., Drechsel, D., Schmid, M. T., Ninkovic, J., Irmler, M., Brill, M. S., Restani, L., Gianfranceschi, L., Cerri, C., Weber, S. N. et al.** (2009). AP2gamma regulates basal progenitor fate in a region- and layer-specific manner in the developing cortex. *Nat. Neurosci.* **12**, 1229-1237.
**Plageman, T. F., Jr, Chung, M. I., Lou, M., Smith, A. N., Hildebrand, J. D., Wallingford, J. B. and Lang, R. A.** (2010). Pax6-dependent Shroom3 expression regulates apical constriction during lens placode invagination. *Development* **137**, 405-415.
**Polleux, F. and Ghosh, A.** (2002). The slice overlay assay: a versatile tool to study the influence of extracellular signals on neuronal development. *Sci. STKE* **2002**, pl9.
**Poulson, N. D. and Lechler, T.** (2010). Robust control of mitotic spindle orientation in the developing epidermis. *J. Cell Biol.* **191**, 915-922.
**Quinn, J. C., Molinek, M., Martynoga, B. S., Zaki, P. A., Faedo, A., Bulfone, A., Hevner, R. F., West, J. D. and Price, D. J.** (2007). Pax6 controls cerebral cortical cell number by regulating exit from the cell cycle and specifies cortical cell identity by a cell autonomous mechanism. *Dev. Biol.* **302**, 50-65.
**Rakic, P.** (2009). Evolution of the neocortex: a perspective from developmental biology. *Nat. Rev. Neurosci.* **10**, 724-735.
**Reillo, I., de Juan Romero, C., Garcia-Cabezas, M. A. and Borrell, V.** (2011). A role for intermediate radial glia in the tangential expansion of the mammalian cerebral cortex. *Cereb. Cortex* **21**, 1674-1694.
**Rieger, M. A., Hoppe, P. S., Smejkal, B. M., Eitelhuber, A. C. and Schroeder, T.** (2009). Hematopoietic cytokines can instruct lineage choice. *Science* **325**, 217-218.
**Saito, T.** (2006). In vivo electroporation in the embryonic mouse central nervous system. *Nat. Protoc.* **1**, 1552-1558.
**Sanada, K. and Tsai, L. H.** (2005). G protein betagamma subunits and AGS3 control spindle orientation and asymmetric cell fate of cerebral cortical progenitors. *Cell* **122**, 119-131.
**Sansom, S. N., Griffiths, D. S., Faedo, A., Kleinjan, D. J., Ruan, Y., Smith, J., van Heyningen, V., Rubenstein, J. L. and Livesey, F. J.** (2009). The level of the transcription factor Pax6 is essential for controlling the balance between neural stem cell self-renewal and neurogenesis. *PLoS Genet.* **5**, e1000511.
**Schmahl, W., Knoedlseder, M., Favor, J. and Davidson, D.** (1993). Defects of neuronal migration and the pathogenesis of cortical malformations are associated with Small eye (Sey) in the mouse, a point mutation at the Pax-6-locus. *Acta Neuropathol.* **86**, 126-135.
**Schwamborn, J. C., Berezikov, E. and Knoblich, J. A.** (2009). The TRIM-NHL protein TRIM32 activates microRNAs and prevents self-renewal in mouse neural progenitors. *Cell* **136**, 913-925.
**Stoykova, A. and Gruss, P.** (1994). Roles of Pax-genes in developing and adult brain as suggested by expression patterns. *J. Neurosci.* **14**, 1395-1412.
**Stoykova, A., Fritsch, R., Walther, C. and Gruss, P.** (1996). Forebrain patterning defects in Small eye mutant mice. *Development* **122**, 3453-3465.
**Stoykova, A., Götz, M., Gruss, P. and Price, J.** (1997). Pax6-dependent regulation of adhesive patterning, R-cadherin expression and boundary formation in developing forebrain. *Development* **124**, 3765-3777.
**Stoykova, A., Treichel, D., Hallonet, M. and Gruss, P.** (2000). Pax6 modulates the dorsoventral patterning of the mammalian telencephalon. *J. Neurosci.* **20**, 8042-8050.
**Stoykova, A., Hatano, O., Gruss, P. and Götz, M.** (2003). Increase in reelin-positive cells in the marginal zone of Pax6 mutant mouse cortex. *Cereb. Cortex* **13**, 560-571.
**Stricker, S. H., Meiri, K. and Götz, M.** (2006). P-GAP-43 is enriched in horizontal cell divisions throughout rat cortical development. *Cereb. Cortex* **16 Suppl. 1**, i121-i131.
**Tamai, H., Shinohara, H., Miyata, T., Saito, K., Nishizawa, Y., Nomura, T. and Osumi, N.** (2007). Pax6 transcription factor is required for the interkinetic nuclear movement of neuroepithelial cells. *Genes Cells* **12**, 983-996.
**Thein, K. H., Kleylein-Sohn, J., Nigg, E. A. and Gruneberg, U.** (2007). Astrin is required for the maintenance of sister chromatid cohesion and centrosome integrity. *J. Cell Biol.* **178**, 345-354.
**Toresson, H., Potter, S. S. and Campbell, K.** (2000). Genetic control of dorsal-ventral identity in the telencephalon: opposing roles for Pax6 and Gsh2. *Development* **127**, 4361-4371.
**Walther, C. and Gruss, P.** (1991). Pax-6, a murine paired box gene, is expressed in the developing CNS. *Development* **113**, 1435-1449.
**Wang, X., Tsai, J. W., Imai, J. H., Lian, W. N., Vallee, R. B. and Shi, S. H.** (2009). Asymmetric centrosome inheritance maintains neural progenitors in the neocortex. *Nature* **461**, 947-955.
**Warren, N., Caric, D., Pratt, T., Clausen, J. A., Asavaritikrai, P., Mason, J. O., Hill, R. E. and Price, D. J.** (1999). The transcription factor, Pax6, is required for cell proliferation and differentiation in the developing cerebral cortex. *Cereb. Cortex* **9**, 627-635.
**Weigmann, A., Corbeil, D., Hellwig, A. and Huttner, W. B.** (1997). Prominin, a novel microvilli-specific polytopic membrane protein of the apical surface of epithelial cells, is targeted to plasmalemmal protrusions of non-epithelial cells. *Proc. Natl. Acad. Sci. USA* **94**, 12425-12430.
**Wilcock, A. C., Swedlow, J. R. and Storey, K. G.** (2007). Mitotic spindle orientation distinguishes stem cell and terminal modes of neuron production in the early spinal cord. *Development* **134**, 1943-1954.
**Wolf, L. V., Yang, Y., Wang, J., Xie, Q., Braunger, B., Tamm, E. R., Zavadil, J. and Cvekl, A.** (2009). Identification of pax6-dependent gene regulatory networks in the mouse lens. *PLoS ONE* **4**, e4159.
**Woodhead, G. J., Mutch, C. A., Olson, E. C. and Chenn, A.** (2006). Cell-autonomous beta-catenin signaling regulates cortical precursor proliferation. *J. Neurosci.* **29**, 12620-12630.
**Wu, S. X., Goebbels, S., Nakamura, K., Nakamura, K., Kometani, K., Minato, N., Kaneko, T., Nave, K. A. and Tamamaki, N.** (2005). Pyramidal neurons of upper cortical layers generated by NEX-positive progenitor cells in the subventricular zone. *Proc. Natl. Acad. Sci. USA* **102**, 17172-17177.
**Yuan, J., Li, M., Wei, L., Yin, S., Xiong, B., Li, S., Lin, S. L., Schatten, H. and Sun, Q. Y.** (2009). Astrin regulates meiotic spindle organization, spindle pole tethering and cell cycle progression in mouse oocyte. *Cell Cycle* **8**, 3384-3395.
**Yun, K., Potter, S. and Rubenstein, J. L.** (2001). Gsh2 and Pax6 play complementary roles in dorsoventral patterning of the mammalian telencephalon. *Development* **128**, 193-205.
**Zhang, J., Woodhead, G. J., Swaminathan, S. K., Noles, S. R., McQuinn, E. R., Pisarek, A. J., Stocker, A. M., Mutch, C. A., Funatsu, N. and Chenn, A.** (2010). Cortical neural precursors inhibit their own differentiation via N-cadherin maintenance of beta-catenin signaling. *Dev. Cell* **18**, 472-479.
**Zheng, Z., Zhu, H., Wan, Q., Liu, J., Xiao, Z., Siderovski, D. P. and Du, Q.** (2010). LGN regulates mitotic spindle orientation during epithelial morphogenesis. *J. Cell Biol.* **189**, 275-288.